

The Promoter Role of Amines in the Condensation of Silicic Acid: A First-Principles Investigation

Xin Liu,* Cai Liu, Zhe Feng, and Changgong Meng*

Cite This: *ACS Omega* 2021, 6, 22811–22819

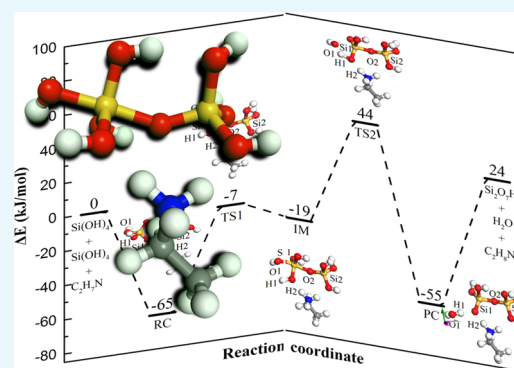
Read Online

ACCESS |

Metrics & More

Article Recommendations

ABSTRACT: Though well-recognized, the molecular-level understanding of the multifunctional roles of amines in the condensation of polysilicic acids, which is one of the key processes in hydrothermal synthesis of zeolites, is still limited. Taking ethylamine as a prototype, we investigated the mechanism of polysilicic acid condensation in the existence of organic amines in aqueous solution with extensive first-principles-based calculations. Because of the high proton affinity, ethylamine exists as amine silicates and alters the subsequent condensation mechanisms from a 1-step lateral attack mechanism accompanied with simultaneous intermolecular proton transfer in neutral aqueous solution to a 2-step S_N2 -like mechanism. Specifically, the 5-coordinated Si species that were not observed on pathways of condensation in neutral solution are effectively stabilized by the ethylamine cations as intermediates, and the barriers for condensation of *ortho*-silicic acid are significantly reduced from 133 kJ/mol in neutral solution to 58 and 63 kJ/mol for formation of the 5-coordinated Si intermediate and proton transfer for water release, respectively. Similar variations of mechanisms and barriers for condensation were also observed in the formation of cyclic trimers as well as linear and cyclic tetramers of *ortho*-silicic acids. Based on these, it was proposed that apart from acting as structure-directing agents, pore fillers, and pH adjusters, organic amines can also function as promoters in the condensation of polysilicic acids.



INTRODUCTION

The hydrothermal synthesis of zeolite is one of the most complicated chemical processes. It involves cascade condensation and hydrolysis of the precursors, mainly polysilicic acids, their solvation and ionization into and precipitation from the reaction mixture, etc.^{1–4} These processes are thermodynamically driven by the bond formation, dissociation, and nonbonding interactions among the reaction species, leading to the formation of zeolite crystallites as the final product, among which the evolution of polysilicic acids is crucial.^{5,6} In principle, the structures, stability, and distribution of polysilicic acids within the reaction mixture would be sensitive to the detailed reaction conditions, including temperature, pH, ingredients, etc.^{7–15} In this sense, understanding the condensation of polysilicic acids at different conditions would be helpful not only for optimization of the zeolite synthesis strategy but also for rationalization of the fabrication approaches with a specific framework structure for desired applications.^{3,4,16}

In zeolite synthesis, the transfer of the precursors into the solution phase, the equilibrium between condensation and hydrolysis of polysilicic acids, and the growth of zeolite crystals are strongly influenced by the pH of the precursor solution.^{1,17–21} Both polysilicic acids and their anions may act as the attacking groups.^{22,23} If the intermolecular proton

transfer takes place prior to the transition state (TS), then the reaction proceeds with an anionic attacking mechanism (AAM) and Si is 4-coordinated in the TS. Another alternative is the silicic acid molecular attacking mechanism (MAM) where Si is 5-coordinated in the TS. In general, the barriers for the AAM (~130 kJ/mol) are ~30 kJ more plausible than those for the MAM.²⁴ As proton transfer is vital, condensation of polysilicic acids is only effective in basic conditions (pH ~11). Alkali metal oxides and hydroxides, organic species, or their combinations are widely used to adjust pH, leading to a high population of silicate anions in the reaction mixture for zeolite synthesis.^{25–30} Therefore, silicate anions were generally considered as the reaction species, and the reactions were simplified as between polysilicic acids and negatively charged silicate anions and were reported plausible through an S_N2 -type mechanism involving formation and dissociation of 5-coordinated Si intermediates.^{22,25,31–35}

Received: June 21, 2021

Accepted: August 18, 2021

Published: August 26, 2021



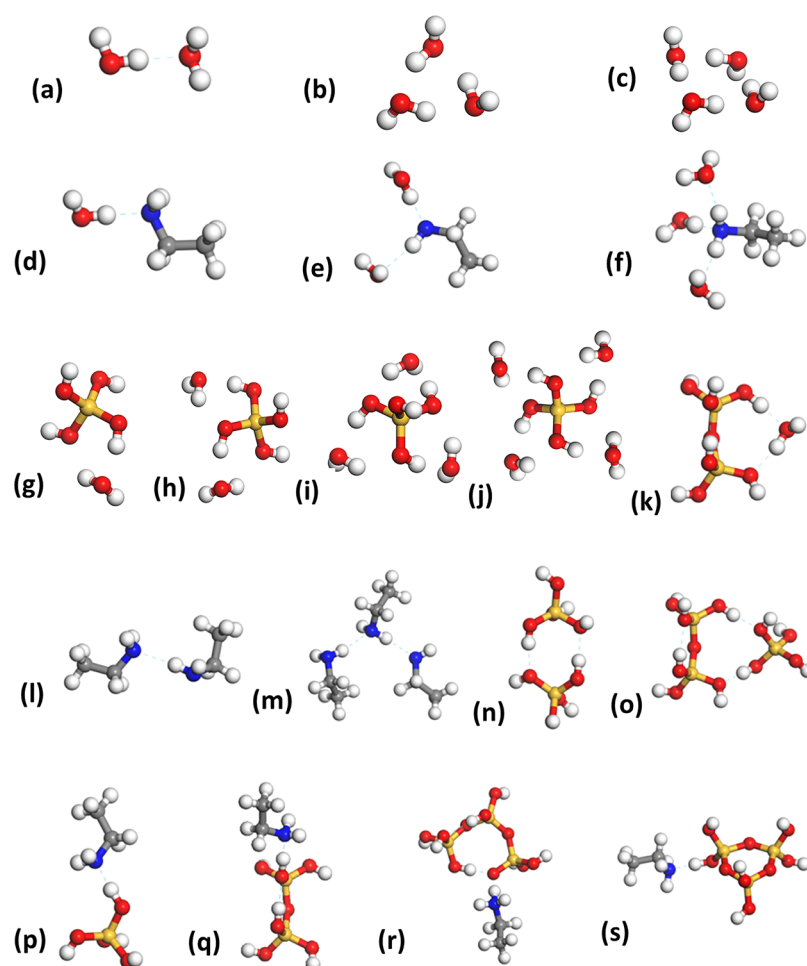


Figure 1. Optimized structures for the hydrogen-bond (HB) complexes formed by water (a–c), water and ethylamine (d–f), *ortho*-silicic acid and water (g–j), disilicic acid and water (k), ethylamine (l,m), between silicic acids (n,o), and between ethylamine and silicic acids (p–s). The Si, O, H, N, and C atoms are in yellow, red, white, blue, and gray, respectively.

Within the past decades, the application of organic species, including amines, etc., to hydrothermal processes enables the controlled synthesis of various inorganic microporous materials with desired framework topologies and chemical composition for various industrial applications.^{3,4,12–16,25,31,36–44} People come to realize the multiple roles of these amines in hydrothermal processes.^{3,25,31,39} Amines have strong affinity to protons and may also shift the pH of the reaction mixture.^{36,45,46} Some amines also act as templates and direct the nucleation of zeolites, and the formed zeolite framework structure can be correlated with the size and shape of these amines. Furthermore, amines within the micropores of the zeolite also function as pore fillers to stabilize the porous structures by forming host–guest interactions.^{40–42} As for the role of amines in the condensation of polysilicic acids, the available reports from Pelster et al.,^{12–15} Kinrade et al.,^{43,44} and Caratzoulas et al.⁴⁷ are still limited to their stabilization of anionic silicate clusters.

Though these pioneer works provided evidence for the multiple roles of amines in the condensation of polysilicic acids, determining the impact of amines on the detailed reaction mechanisms, specifically the variation of the role of the 5-coordinated Si species on the reaction pathways from a transition state in neutral aqueous solution to an intermediate, remains challenging. We investigate the role of amines in the condensation of polysilicic acids by extensive first-principles-

based calculations and proposed that apart from acting as structure-directing agents, pore fillers, and pH adjusters, amines can also behave as promoters in the condensation of polysilicic acids.

RESULTS AND DISCUSSION

The interactions among species within the reaction mixture, namely, ethylamine, polysilicic acids, and water, would have an important impact on their forms of existence and potential reactions among them. We firstly investigated the most stable complexes formed among these species to estimate their potential interactions to deduce the potential evolution of polysilicic acids (Figure 1 and Table 1).

HB complexes may be formed among water molecules. The length of hydrogen bonds falls in the range from 1.80 to 1.90 Å. The calculated ΔE in solution are -20 , -40 , and -81 kJ/mol, respectively, for the dimer (Figure 1a), trimer (Figure 1b), and tetramer (Figure 1c). ΔE for the water dimer, trimer, and tetramer in the gas phase were also calculated to be -21 , -65 , and -118 kJ/mol, respectively, and compared well with the previous results (routes a–c, Table 1).⁴⁸ It should be noted that the calculated ΔE for the water dimer in the gas phase is in reasonable agreement with the experimental finding of -22.76 ± 2.93 kJ/mol⁴⁹ and the value of -20.8 kJ/mol at the MP2/CBS level.⁵⁰ Our estimated BSSE for the gas-phase water

Table 1. The Change in Total Energy (ΔE) and Enthalpies (ΔH) in kJ/mol, for Formation of Complexes among Water, Polysilicic Acid, and Ethylamine Molecules at 298 and 450 K in Aqueous Solution

route	reactions	ΔE^a (kJ/mol)	ΔE^b (kJ/mol)	ΔH_{298K}^c (kJ/mol)	ΔH_{450K}^d (kJ/mol)	BSSE ^e (kJ/mol)
a	$2H_2O \rightarrow (H_2O)_2$	-20(-8)	-20(-8)	-12	-11	-1.4
b	$3H_2O \rightarrow (H_2O)_3$	-40(-11)	-40(-14)	-23	-23	-2.8
c	$4H_2O \rightarrow (H_2O)_4$	-81(-41)	-81(-42)	-55	-55	-3.4
d	$C_2H_5NH_2 + H_2O \rightarrow C_2H_5NH_2(H_2O)$	-23(-13)		-17	-16	-1.8
e	$C_2H_5NH_2 + 2H_2O \rightarrow C_2H_5NH_2(H_2O)_2$	-25(-20)		-12	-9	-2.4
f	$C_2H_5NH_2 + 3H_2O \rightarrow C_2H_5NH_2(H_2O)_3$	-26(-25)		-8	-2	-3.1
g	$Si(OH)_4^d + H_2O \rightarrow Si(OH)_4(H_2O)$	-19(-9)	-19(-8)	-12	-10	-2.2
h	$Si(OH)_4 + 2H_2O \rightarrow Si(OH)_4(H_2O)_2$	-41(-8)	-40(-9)	-18	-16	-2.3
i	$Si(OH)_4 + 3H_2O \rightarrow Si(OH)_4(H_2O)_3$	-62(-9)	-63(-10)	-27	-23	-2.1
j	$Si(OH)_4 + 4H_2O \rightarrow Si(OH)_4(H_2O)_4$	-84(-14)	-88(-10)	-36	-30	-3.0
k	$Si_2O(OH)_6^d + H_2O \rightarrow Si_2O(OH)_6(H_2O)$	-34(-8)	-33(-10)	-18	-17	-2.3
l	$2C_2H_5NH_2 \rightarrow (C_2H_5NH_2)_2$	-2(6)		5	7	-1.3
m	$3C_2H_5NH_2 \rightarrow (C_2H_5NH_2)_3$	-3(9)		10	14	-2.2
n	$2Si(OH)_4 \rightarrow (Si(OH)_4)_2$	-28(-15)	-30(-20)	-20	-21	-2.5
o	$Si(OH)_4 + Si_2O(OH)_6^d \rightarrow Si(OH)_4 \cdot Si_2O(OH)_6$	-29(-13)	-31(-18)	-20	-22	-2.3
p	$Si(OH)_4 + C_2H_5NH_2 \rightarrow Si(OH)_4 \cdot C_2H_5NH_2$	-35(-26)		-28	-27	-2.2
q	$Si_2O(OH)_6^d + C_2H_5NH_2 \rightarrow Si_2O(OH)_6 \cdot C_2H_5NH_2$	-40(-24)		-35	-35	-2.8
r	$Si_3O_2(OH)_8^d + C_2H_5NH_2 \rightarrow Si_3O_2(OH)_8 \cdot C_2H_5NH_2$	-48(-38)		-38	-38	-2.6
s	$Si_4O_4(OH)_8^d + C_2H_5NH_2 \rightarrow Si_4O_4(OH)_8 \cdot C_2H_5NH_2$	-40(-29)		-35	-34	-2.6

^aReaction energy, calculated as the energy difference between reactants and products. According to ref 57, the BSSE for the BLYP/DNP calculations would be rather small, so we did not correct the ΔE with BSSE. The numbers in parentheses were corrected with ZPE. ^bResults mentioned in ref 48, the numbers in parentheses were corrected with ZPE. ^cThe formation enthalpy change, calculated as the difference in enthalpy between reactants and products, corrected with ZPE at 298 and 450 K, respectively. ^d $C_2H_5NH_2$, $Si(OH)_4$, $Si_2O(OH)_6$, $Si_3O_2(OH)_8$, and $Si_4O_4(OH)_8$ represent ethylamine, the monomer, dimer, linear trimer, and cyclic trimer of *ortho*-silicic acid, respectively. ^eCalculated BSSE correction in vacuum to the interactions in the formed complexes.

dimer is 1.4 kJ/mol and is in reasonable agreement with previous reports.^{48,51} The calculated BSSE in vacuum for structures in Figure 1 can be found in Table 1. The calculated BSSEs for all structures are less than 3 kJ/mol per interaction. In this sense, the proposed theoretical approach would be adequate to investigate the condensation of silicic acids.

Ethylamine may also form a monohydrate (Figure 1d), dihydrate (Figure 1e), and trihydrate (Figure 1f) in solution. Due to the difference in proton affinity, ethylamine acts as an HB acceptor to interact with surrounding water molecules. These complexes are plausible with a N—H distance of 1.83 Å, and the calculated ΔE are approximately -23 kJ/mol. ΔE would vary within 3 kJ/mol when additional water molecules act as HB acceptors (routes d–f, Table 1).

Water can also interact with *ortho*-silicic acid to form a monohydrate, dihydrate, trihydrate, and tetrahydrate. Similarly, disilicic acid can also form monohydrate, as well as other HB complexes with water (Figure 1g–k). Among these complexes, only those with water acting as HB acceptors are plausible, and this can be explained by the large pK_a of silicic acids. The calculated exothermicity for the monohydrate of *ortho*-silicic acid is -19 kJ/mol, and the averaged ΔE for formation of the monohydrate, dihydrate, trihydrate, and tetrahydrate are -19, -20, -20, and -21 kJ/mol, respectively (routes g–j, Table 1). As water acts as both an HB acceptor and donor (Figure 1k), the calculated ΔE for the complex formed between a disilicic acid and water is -34 kJ/mol (route k, Table 1) and is more significant than that for *ortho*-silicic acid monohydrate. The calculated ΔE and ΔH at 298 and 450 K are in good agreement with previous results.⁴⁸ Different from the hydrated silicic acids, the calculated ΔE for the ethylamine dimer and trimer (Figure 1l,m, routes l and m, Table 1) are only -2 and

-3 kJ/mol, suggesting their low population in the reaction mixture.

We then moved on to investigate the HB complexes formed among silicic acids. *ortho*-Silicic acid would act as an HB acceptor to form complexes, such as a dimer (Figure 1n) and a 2–1 complex (Figure 1o) as it has higher proton affinity according to the free energy change for deprotonation (-63 vs -95 kJ/mol).^{22,24,52} The calculated ΔE for the dimer and the 2–1 complex are -28 and -29 kJ/mol, respectively (routes n and o, Table 1), and the difference in ΔE can be explained with the number of HBs in the complexes.

The interactions among polysilicic acids and ethylamine (Figure 1p–s and routes p–s, Table 1) were also investigated. In the most plausible structures of these complexes, ethylamine acts as the HB acceptor to interact with polysilicic acids at N—H distances of ~1.60 Å, suggesting both the ionization of ethylamine and the strong binding between the amine and the acids. The calculated ΔE for these complexes formed from *ortho*-silicic acid, a dimer, and linear and cyclic trimers with ethylamine are -35, -40, -48, and -40 kJ/mol, respectively (Figure 1p–s).

According to ΔE , the complexes formed between polysilicic acids and ethylamine are the most plausible. The complexes formed among polysilicic acids rank the second and are superior to those formed between water and polysilicic acids and ethylamine. Considering the significant role of proton transfer in the reaction mechanism and thermodynamics,²⁴ the formation of amine cations and polysilicate anions in the reaction solution may further promote the condensation of polysilicic acids.

We moved on to investigate the condensation mechanism of *ortho*-silicic acid in the existence of ethylamine. In the existence of ethylamine (RC, Figure 2), the amine accepts the proton

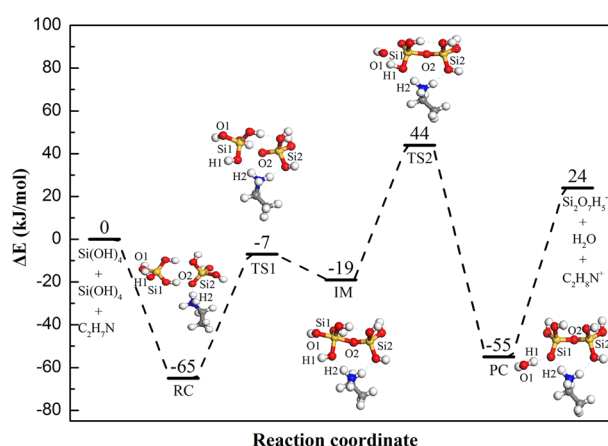


Figure 2. Potential energy surface condensation of two *ortho*-silicic acid molecules in the existence of ethylamine. The Si, O, H, N, and C atoms are in yellow, red, white, blue, and gray, respectively.

from one of the *ortho*-silicic acids, making the corresponding O (O2) more naked as the negatively charged approaching group to Si1 for formation of the Si1–O2–Si2 bond. In this structure, the O2–Si1 distance is 3.71 Å, and the O2–H1 distance is 1.60 Å, suggesting the enhanced hydrogen bonding between the silicic acids. However, the O2–H2 distance increases to 1.53 Å, suggesting the potential of proton transfer. The newly formed N–H2 distance is 1.10 Å and, though longer than the calculated N–H distance in ethylammonium cations of 1.03 Å, can still be considered as evidence for formation of ethylamine *ortho*-silicate. Both the enhanced hydrogen bonds and the conversion of silicic acid into amine silicate make the formation of RC (Figure 2) more exothermic by ~30 kJ/mol as compared to ethylamine *ortho*-silicate (–60 vs –35 kJ/mol, Figure 1p). This is in excellent agreement with the observed high stability of amine silicates in aqueous solution and the gas phase.^{12–15,43,44,47}

Starting with RC, the electrostatic interaction between naked and negatively charged O2 due to proton transfer to ethylamine and positively charged Si1 drives the further movement of O2 to Si1 to reach TS1 (TS1, Figure 2). During this 58 kJ/mol energy uphill process, the O2–Si1 distance decreases from 3.71 Å in RC to 2.36 Å, showing the strengthening of O2–Si1 interaction. At the same time, the ethylamine cation rotates slightly forming HB with O connected with H1. In this way, the O2–H2 distance is increased from 1.53 to 2.67 Å, implying that the completion of proton transfer to ethylamine takes place. This leads to charge accumulation at O2 and a decrease in the Si2–O2 distance to 1.59 Å. The O1–H1 distance also decreases to 2.48 Å, showing the transfer of H1 to O1, and the O1–Si1 distance is extended from 1.67 to 1.70 Å due to the change of coordination on Si1.

The further energy downhill process connects TS1 with the 5-coordinated Si intermediate (IM). The Si1–O2 distance decreases to 1.86 Å during formation of the 5-coordinated Si species. This process does not involve the change of coordination around Si2, so the Si2–O2 distance is retained. Due to the overcoordination at Si1, the O1–H1 distance decreases to 2.28 Å, and the Si1–O1 distance increases to 1.77 Å. The tendency for proton transfer to O1 for formation of a water molecule to detach from Si1 to reach the plausible 4-coordinated Si structure is obvious. The results from vibrational frequency and intrinsic reaction coordinate (IRC)

calculations confirmed that IM is a local minimum connected to TS1. The exothermicity for formation of IM is only –12 kJ/mol with respect to TS1. This is in reasonable agreement with the reaction thermodynamics reported by Prosenec et al. where they found that the exothermicity for formation of the 5-coordinated Si species is about –18 kJ/mol from *ortho*-silicic acid anions and acid, according to the corresponding transition state.⁵³ The small exothermicity also implies the instability of IM and can be ascribed to the overcoordination at Si1. However, as 5-coordinated Si is effectively stabilized by amine cations and the HB network among the reaction species, this instability is well-balanced, and IM exists as an intermediate.

Also originated from the instability of 5-coordinated Si1 in IM and the tendency for proton transfer of H1 to O1 for water formation and detachment from Si1 to reach the most plausible 4-coordination, the further reaction connects IM with the ethylamine salt of the dimer of *ortho*-silicic acid as the final product (PC, Figure 2). In TS2 (TS2, Figure 2), the Si1–O2 distance decreases to 1.74 Å, which is typical in zeolites and polysilicic acids, the O1–H1 distance decreases to 1.29 Å, and the Si1–O1 distance is elongated to 2.23 Å. These structure changes highlight the simultaneous proton transfer for formation of water molecules, the detachment of the formed water molecules, and the strengthening of the Si1–O1 bond. The calculated reaction barrier for this process is 63 kJ/mol, and PC is exothermic by 99 and 36 kJ/mol with respect to IM and TS2, respectively. After TS2, the O1–H1 distance is further shortened to 0.98 Å, and the Si1–O1 distance increases to 3.90 Å. In this sense, the formed water molecule is completely detached from Si1. As the coordination at Si2 and around the ethylamine is not changed, the structure of related parts of the reaction species does not vary significantly. Due to the electrostatic interaction in the formed ethylamine silicate and the hydrogen bonds with water, further evolution of PC into disilicate anions and ethylamine cations in aqueous solution would be endothermic by 74 kJ/mol.

The condensation mechanism was also investigated with the B3LYP hybrid functional.⁵⁴ In these calculations, the dispersion interactions were handled with the scheme developed by Grimme⁵⁵ and implemented by Reuter et al.⁵⁶ The results are essentially the same. The calculated energy barriers at TS1 and TS2 are 41 and 71 kJ/mol, respectively, while the formation of IM is 11 kJ/mol exothermic with respect to TS1. These are in reasonable agreement with the aforementioned energetics calculated with the BLYP functional, and the difference in energy barriers can be attributed to the treatment of dispersion interactions and correlation functions.⁵⁶

For comparison, the condensation mechanism of *ortho*-silicic acid without ethylamine was also reinvestigated. In agreement with a previous report, the condensation proceeds with proton transfer, formation of the Si–O–Si bond, and detachment of water in a single-step mechanism with a 5-coordinated Si as the TS, and the reaction barrier is 133 kJ/mol.²⁴ In this sense, ethylamine stabilizes 5-coordinate Si-species and alters the reaction pathway to a 2-step mechanism with significantly decreased reaction barriers of 58 and 63 kJ/mol, respectively, for formation of and water detachment from the 5-coordinate Si intermediate.

To generalize the findings, the condensation between linear trisilicic acid and *ortho*-silicic acid was also investigated (Figure 3). The calculated reaction barriers for formation of the 5-coordinated Si species and water formation and detachment

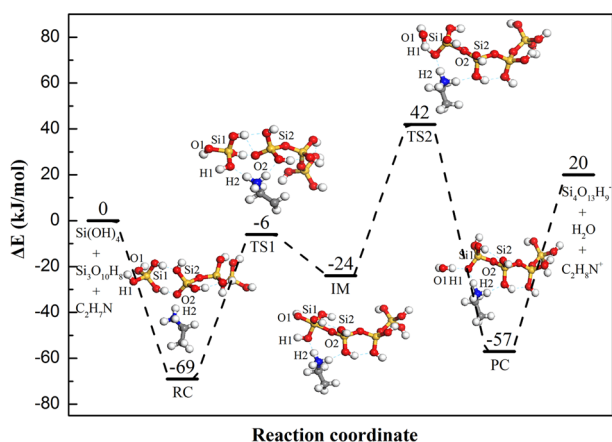


Figure 3. Potential energy surface of condensation between a trimer and a monomer of *ortho*-silicic acid molecules in the existence of ethylamine. The Si, O, H, N, and C atoms are in yellow, red, white, blue, and gray, respectively.

during the reaction between trisilicic acid and *ortho*-silicic acid are 63 and 66 kJ/mol, respectively. These values compare well with the aforementioned barriers for the reaction between two *ortho*-silicic acid molecules (58 and 63 kJ/mol, respectively, for formation of the 5-coordinated Si species and water formation and detachment).

We also investigated the mechanism of the intramolecular condensation of linear trisilicic acid in the existence of ethylamine (Figure 4). Similar to the case for dimerization of

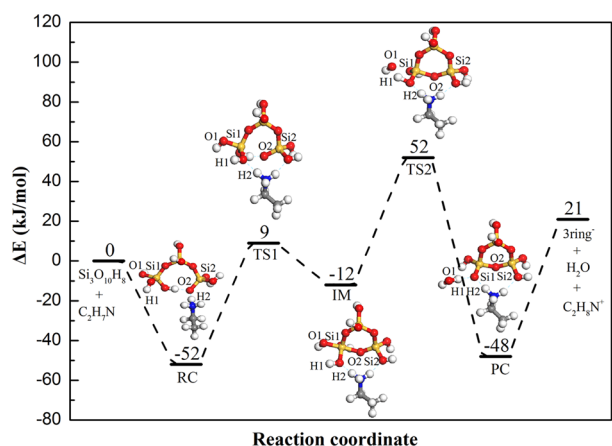


Figure 4. Potential energy surface for formation of a cyclic trimer from a linear trimer of *ortho*-silicic acid in the existence of ethylamine. The Si, O, H, N, and C atoms are in yellow, red, white, blue, and gray, respectively.

ortho-silicic acid, the linear trimer adapts a cyclic conformation to facilitate the formation of hydrogen bonds. In the existence of ethylamine, the ethylamine takes the proton originally attached to the linear trisilicic acid, leading to the formation of RC (RC, Figure 4). In RC, the approaching O (O2) is still 3.61 Å from Si1, while the Si2–O2 and Si1–O1 distances are 1.61 and 1.66 Å and are right in the range of conventional Si–O distances in polysilicic acids. However, the H2–O2 is elongated to 1.52 Å, while the H2–N distance decreases to 1.11 Å, confirming the proton transfer for formation of ethylammonium cations. The results of frequency calculation confirmed that RC is a stable species and its formation is 52

kJ/mol exothermic with respect to freestanding linear trisilicic acid in the cyclic hydrogen bonded conformation and ethylamine in aqueous solution. The electrostatic interaction drives naked and negatively charged O2 to approach Si1 to reach the transition state (TS1, Figure 4). In this 61 kJ/mol energy uphill process, the Si1–O2 distance decreases from 3.61 to 2.71 Å, and the O2–H2 distance increases to 2.60 Å, showing the tendency for simultaneous breaking of the O2–H2 bond and formation of Si1–O2 bonds. The slight reorientation of the ethylammonium cation was also observed, with the formation of two hydrogen bonds with the two terminal –OH groups (TS1, Figure 4). Due to the change of the coordination environment around Si1, the O1–H1 distance is also shortened from 3.01 to 2.62 Å in TS1. The further strengthening of the Si1–O2 bonds leads to the formation of the 5-coordinated Si intermediate (IM, Figure 4). In IM, the Si1–O2 distance further decreases from 2.37 Å in TS1 to 1.84 Å, while the Si2–O2 distance remains at 1.61 Å as there is no significant coordination change around Si2. The H2 that transferred from O2 is now oriented to form HB with the O atom where H1 is attached to, and the O2–H2 distance increases to 2.81 Å. Due to the newly formed hydrogen bond, the O1–H1 distance also decreases to 2.26 Å, and the Si1–O1 increases to 1.76 Å. The subsequent reaction proceeds with the proton transfer of H1 to O1 for water formation as the detaching group from Si1. In TS2 (TS2, Figure 4), the O1–H1 distance is further shortened to 1.29 Å and is a typical strong hydrogen bond. The ethylamine cation forms a hydrogen bond with the O atom originally holding H1 and stabilized the transition state for proton transfer. The Si1–O2 distance decreases further to 1.74 Å, and the Si1–O1 distance increases to 2.20 Å, showing the simultaneous proton transfer for formation of detaching water and the reorganization of the coordination around Si1. Due to the proton transfer and formation of Si–O bonds, the reaction is 100 kJ/mol exothermic with respect to TS2, leading to the formation of ethylammonium cations with an attached water molecule as products (PC, Figure 4). With the same approach, the mechanism for formation of cyclic tetrasilicic acid from linear tetrasilicic acid was also investigated (Figure 5), yielding exactly the same results.

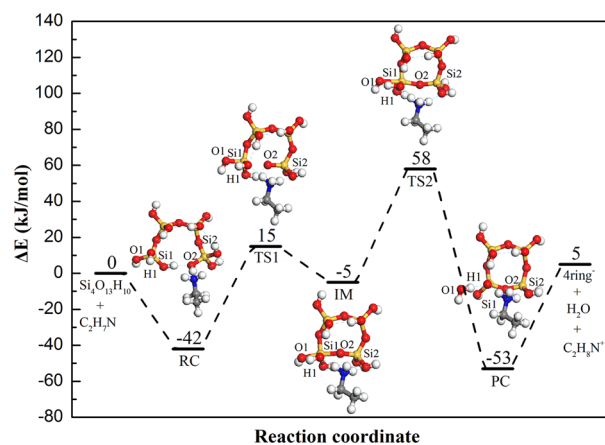


Figure 5. Potential energy surface for formation of a cyclic tetramer from a linear tetramer of *ortho*-silicic acid in the existence of ethylamine. The Si, O, H, N, and C atoms are in yellow, red, white, blue, and gray, respectively.

It is worth noting that the formation of RCs as reaction species is strongly exothermic. The exothermicities are 65, 69, 52, and 42 kJ/mol for formation of RCs on pathways to dimer, linear tetramer, cyclic trimer, and tetramer amine silicates, respectively. The large exothermicity can be attributed to the proton transfer to ethylamine, which effectively stabilizes the polysilicic acid in the form of ethylamine silicates, while the slight difference in exothermicity can be attributed to the proton-donating ability of the silicic acids as well as the hydrogen bond network. On the other hand, the barriers for formation of 5-coordinated Si intermediates on the pathways for formation of linear and cyclic oligomers of polysilicic acid in the existence of ethylamine are 58, 63, 61, and 57 kJ/mol, respectively, while the barriers for proton transfer for water detachment are 63, 64, 64, and 63 kJ/mol, respectively, on pathways to the dimer, linear tetramer, cyclic trimer, and tetramer. The TSs for formation of 5-coordinated Si intermediates are also stabilized by amine cations that interact with silicic acids through the hydrogen bond network and brings both the reacting moieties together. In this sense, the formation of 5-coordinated Si intermediates is dependent on the structures of the silicic acids, and there is a difference of ~ 10 kJ/mol in reaction barriers between the linear and cyclic oligomers. However, the barriers for dissociation of intermediates are very similar. A close examination of the TSs for proton transfer and water release shows that these TSs actually correspond to proton transfer among $-OH$ s attached to Si1. This finely explains the reported molecular dynamics simulation results that cations in the reaction mixture have less impact on the proton transfer for detaching of the formed water.^{7–11} Further to these, in the formation of final products, the amine polysilicates are all exothermic with respect to the 5-coordinated Si intermediates, and the exothermicities are 33, 36, 33, and 48 kJ/mol, respectively, on the pathways to the dimer, linear tetramer, cyclic trimer, and tetramer of *ortho*-silicic acid. These are also in reasonable agreement with the experimentally observed high stability of amine silicate in both solution and the gas phase.^{12–15,43,44,47}

As organic amines may also get protonized with water in the reaction mixture and release OH^- and zeolites are generally synthesized at $pH > 11$, the potential roles of OH^- in the condensation of *ortho*-silicic acid were also investigated and compared. Similar to organic amines (Figure 2), OH^- can also harvest protons from *ortho*-silicic acid, leading to the formation of hydrogen bonded silicic acid–silicate ion as the reaction complex. However, the calculated barrier for formation of the 5-coordinated Si intermediate increases from 58 with ethylamine to 73 kJ/mol with OH^- , while that for proton transfer for water release increases from 63 to 80 kJ/mol (Figure 2). A similar increase was observed in reaction barriers calculated with the B3LYP functional with dispersion interaction treated with the approach developed by Grimme. The barriers for formation of 5-coordinated Si intermediate and proton transfer in the existence of OH^- are 63 and 94 kJ/mol, respectively, and are significantly larger than those values with involvement of ethylamine (41 and 71 kJ/mol, respectively at the B3LYP level). As the reaction mechanism for condensation is also 2-step with 5-coordinated Si species as the intermediate and the barriers are lower than those in neutral solution, OH^- may also promote the condensation. The differences in reaction barriers can be attributed to the different proton affinity of ethylamine and OH^- and also suggest that OH^- is not as effective as ethylamine in promoting the condensation of silicic acids. To

this end, the ethylamine in the reaction mixture converts the silicic acids into amine silicates, alters the reaction thermodynamics and reaction paths by efficiently stabilizing the reaction species, turns the 5-coordinated Si species into intermediates, and thus promotes the condensation of polysilicic acids.

CONCLUSIONS

We investigated the mechanism of polysilicic acid condensation in the existence of ethylamine in aqueous solution with extensive first-principles-based calculations to highlight the multifunctional role of amines in the condensation of polysilicic acids. Due to the strong proton affinity of amines, the formation reactions of RCs as reaction species are strongly exothermic. The amines effectively stabilize the 5-coordinated Si species as intermediates and turn the reaction mechanism from a 1-step lateral attack mechanism accompanied with simultaneous intermolecular proton transfer in neutral aqueous solution to a 2-step S_N2 -like mechanism. The barriers to 5-coordinated Si intermediates on the pathways for formation of linear and cyclic oligomers of polysilicic acid in the existence of ethylamine are 58, 63, 61, and 57 kJ/mol. As the condensation terminates with proton transfer between hydroxyls on the 5-coordinated Si intermediate, it is less structure-dependent. However, there is a weak dependence of ~ 10 kJ/mol on the formation of the 5-coordinated Si intermediate on the structure of silicic acids. As ethylamine effectively stabilizes the reaction species turning the 5-coordinated Si species into intermediates and significantly lowers the reaction barrier, we proposed that apart from acting as structure-directing agents, pore fillers, and pH adjusters, organic amines also function as promoters in the condensation of polysilicic acids.

THEORETICAL METHODS

The condensation mechanisms of polysilicic acids in the existence of ethylamine in aqueous solution were investigated by first-principles-based calculations. Unless specified, all the calculations were performed with the Becke, Lee, Yang, and Parr (BLYP) functional within the formalism of generalized gradient approximation.^{57,58} The full-electron double numerical plus polarization basis set (DNP) version 3.5 was used to describe the ground-state electronic structures of amine, polysilicic acids, water, and complexes formed among them.⁵⁷ The used combination of the BLYP and the DNP basis set was widely used previously in investigations on the condensation of polysilicic acids, nucleation and growth of zeolites, etc.,^{25,31–34,39,48,52} while the reported results in terms of transition states and reaction isotherms are in reasonable agreement with those obtained with other combinations of functionals and basis sets.^{7,8,10,11,22,23,29,59–63} As all electronic states of C, N, O, Si, and H were treated with numerical basis sets of at least double-zeta quality,⁵⁷ the calculated energies are expected to exhibit small basis set superposition errors (BSSEs), together with a reasonable description of weak bonds, although still within the limits of the DFT framework.^{48,51} Our calculated BSSE for the water dimer in the gas phase is 1.4 kJ/mol. In all these calculations, an orbital cutoff of 4.6 Å was used, and the solvation effect was handled with the COSMO model.^{64–66} Combinations of linear and quadratic synchronous transit methods were used to trace the TSs on the reaction potential energy surface.⁶⁷ Further TS optimization and frequency calculations were performed to confirm these TSs. The enthalpy change (ΔH) of a reaction was evaluated as

the difference in enthalpy between the reactants and the products at 298 and 450 K according to eqs 1–5.^{68,69} The reported energy change (ΔE) was corrected with zero point energy (ZPE). All the calculations were performed with the DMol³ code.^{70,71}

$$\Delta H(T) = H_{\text{product}}(T) - H_{\text{reactant}}(T) \quad (1)$$

$$H(T) = E_{\text{elect}} + E_{\text{vib}}(T) + E_{\text{rot}}(T) + E_{\text{trans}}(T) + RT \quad (2)$$

$$E_{\text{trans}}(T) = \frac{3}{2}RT \quad (3)$$

$$E_{\text{rot}}(T) = \frac{3}{2}RT \quad (4)$$

$$E_{\text{vib}}(T) = \frac{R1}{k2} \sum_i h\nu_i + \frac{R}{k} \sum_i \frac{h\nu_i \exp\left(-\frac{h\nu_i}{kT}\right)}{\left[1 - \exp\left(-\frac{h\nu_i}{kT}\right)\right]} \quad (5)$$

In eqs 1–5, $H_{\text{product}}(T)$ and $H_{\text{reactant}}(T)$ are the enthalpy of the product and the reactant at a specific temperature, respectively, k is Boltzmann's constant, h is Planck's constant, and ν_i are the vibrational frequencies of the i^{th} normal modes.

AUTHOR INFORMATION

Corresponding Authors

Xin Liu – State Key Laboratory of Fine Chemicals and Department of Chemistry, Dalian University of Technology, Dalian 116024, P. R. China; orcid.org/0000-0002-4422-4108; Email: xliu@dlut.edu.cn

Changgong Meng – State Key Laboratory of Fine Chemicals and Department of Chemistry, Dalian University of Technology, Dalian 116024, P. R. China; orcid.org/0000-0003-1662-0565; Email: cgmeng@dlut.edu.cn

Authors

Cai Liu – State Key Laboratory of Fine Chemicals and Department of Chemistry, Dalian University of Technology, Dalian 116024, P. R. China

Zhe Feng – State Key Laboratory of Fine Chemicals and Department of Chemistry, Dalian University of Technology, Dalian 116024, P. R. China

Complete contact information is available at:

<https://pubs.acs.org/10.1021/acsomega.1c03235>

Author Contributions

X.L. designed this research and drafted the manuscript. X.L. and C.M. contributed materials and analysis tools. C.L. performed the theoretical calculations and is responsible for the results presented. The manuscript was written through contributions of all authors. All authors have given approval to the final version of the manuscript.

Notes

The authors declare no competing financial interest.

ACKNOWLEDGMENTS

This work was supported by the National Natural Science Foundation of China (NSFC, nos. 21771029, 11811530631, and 21573034). The computation time was provided by the Supercomputer Center at Dalian University of Technology.

REFERENCES

- (1) Li, R.; Chawla, A.; Linares, N.; Sutjianto, J. G.; Chapman, K. W.; Martinez, J. G.; Rimer, J. D. Diverse Physical States of Amorphous Precursors in Zeolite Sol Gel Syntheses. *Ind. Eng. Chem. Res.* **2018**, *57*, 8460–8471.
- (2) Li, C.; Moliner, M.; Corma, A. Building Zeolites from Precrystallized Units: Nanoscale Architecture. *Angew. Chem., Int. Ed.* **2018**, *57*, 15330–15353.
- (3) Li, J.; Corma, A.; Yu, J. Synthesis of new zeolite structures. *Chem. Soc. Rev.* **2015**, *44*, 7112–7127.
- (4) Li, Y.; Cao, H.; Yu, J. Toward a New Era of Designed Synthesis of Nanoporous Zeolitic Materials. *ACS Nano* **2018**, *12*, 4096–4104.
- (5) Kumar, A.; Molinero, V. Two-Step to One-Step Nucleation of a Zeolite through a Metastable Gyroid Mesophase. *J. Phys. Chem. Lett.* **2018**, *9*, 5692–5697.
- (6) Kumar, A.; Nguyen, A. H.; Okumu, R.; Shepherd, T. D.; Molinero, V. Could Mesophases Play a Role in the Nucleation and Polymorph Selection of Zeolites? *J. Am. Chem. Soc.* **2018**, *140*, 16071–16086.
- (7) Trinh, T. T.; Jansen, A. P. J.; van Santen, R. A.; VandeVondele, J.; Meijer, E. J. Effect of Counter Ions on the Silica Oligomerization Reaction. *ChemPhysChem* **2009**, *10*, 1775–1782.
- (8) Zhang, X. Q.; Trinh, T. T.; van Santen, R. A.; Jansen, A. P. J. Structure-Directing Role of Counterions in the Initial Stage of Zeolite Synthesis. *J. Phys. Chem. C* **2011**, *115*, 9561–9567.
- (9) Pavlova, A.; Trinh, T. T.; van Santen, R. A.; Meijer, E. J. Clarifying the role of sodium in the silica oligomerization reaction. *Phys.Chem.Chem.Phys.* **2013**, *15*, 1123–1129.
- (10) Trinh, T. T.; Tran, K. Q.; Zhang, X. Q.; van Santen, R. A.; Meijer, E. J. The role of a structure directing agent tetramethylammonium template in the initial steps of silicate oligomerization in aqueous solution. *Phys.Chem.Chem.Phys.* **2015**, *17*, 21810–21818.
- (11) Trinh, T. T.; Rozanska, X.; Delbecq, F.; Sautet, P. The initial step of silicate versus aluminosilicate formation in zeolite synthesis: a reaction mechanism in water with a tetrapropylammonium template. *Phys.Chem.Chem.Phys.* **2012**, *14*, 3369–3380.
- (12) Pelster, S. A.; Kalamajka, R.; Schrader, W.; Schuth, F. Monitoring the nucleation of zeolites by mass spectrometry. *Angew. Chem., Int. Ed.* **2007**, *46*, 2299–2302.
- (13) Pelster, S. A.; Schrader, W.; Schuth, F. Monitoring temporal evolution of silicate species during hydrolysis and condensation of silicates using mass spectrometry. *J. Am. Chem. Soc.* **2006**, *128*, 4310–4317.
- (14) Pelster, S. A.; Weimann, B.; Schaack, B. B.; Schrader, W.; Schuth, F. Dynamics of silicate species in solution studied by mass spectrometry with isotopically labeled compounds. *Angew. Chem., Int. Ed.* **2007**, *46*, 6674–6677.
- (15) Schaack, B. B.; Schrader, W.; Schüth, T. Detection of Structural Elements of Different Zeolites in Nucleating Solutions by Electro-spray Ionization Mass Spectrometry. *Angew. Chem., Int. Ed.* **2008**, *47*, 9092–9095.
- (16) Dusselier, M.; Davis, M. E. Small-Pore Zeolites: Synthesis and Catalysis. *Chem. Rev.* **2018**, *118*, 5265–5329.
- (17) Fleming, B. A.; Crerar, D. A. Silicic acid ionization and calculation of silica solubility at elevated temperature and pH application to geothermal fluid processing and reinjection. *Geothermics* **1982**, *11*, 15–29.
- (18) Chan, S. H. A review on solubility and polymerization of silica. *Geothermics* **1989**, *18*, 49–56.
- (19) Sefcik, J.; McCormick, A. V. Thermochemistry of aqueous silicate solution precursors to ceramics. *AIChE J.* **1997**, *43*, 2773–2784.
- (20) Niibori, Y.; Kunita, M.; Tochiyama, O.; Chida, T. Dissolution Rates of Amorphous Silica in Highly Alkaline Solution. *J. Nucl. Sci. Technol.* **2000**, *37*, 349–357.
- (21) Hu, T.; Gao, W.; Liu, X.; Zhang, Y.; Meng, C. Synthesis of zeolites Na-A and Na-X from tablet compressed and calcinated coal fly ash. *R. Soc. Open Sci.* **2017**, *4*, 170921.

- (22) Trinh, T. T.; Jansen, A. P. J.; van Santen, R. A. Mechanism of oligomerization reactions of silica. *J. Phys. Chem. B* **2006**, *110*, 23099–23106.
- (23) Moqadam, M.; Riccardi, E.; Trinh, T. T.; Lervik, A.; van Erp, T. S. Rare event simulations reveal subtle key steps in aqueous silicate condensation. *Phys. Chem. Chem. Phys.* **2017**, *19*, 13361–13371.
- (24) Liu, X.; Liu, C.; Meng, C. Oligomerization of Silicic Acids in Neutral Aqueous Solution: A First-Principles Investigation. *Int. J. Mol. Sci.* **2019**, *20*, 3037.
- (25) Mora-Fonz, M. J.; Catlow, C. R. A.; Lewis, D. W. Modeling aqueous silica chemistry in alkali media. *J. Phys. Chem. C* **2007**, *111*, 18155–18158.
- (26) Rollmann, L. D.; Schlenker, J. L.; Lawton, S. L.; Kennedy, C. L.; Kennedy, G. J.; Doren, D. J. On the role of small amines in zeolite synthesis. *J. Phys. Chem. B* **1999**, *103*, 7175–7183.
- (27) Rollmann, L. D.; Schlenker, J. L.; Kennedy, C. L.; Kennedy, G. J.; Doren, D. J. On the role of small amines in zeolite synthesis. 2. *J. Phys. Chem. B* **2000**, *104*, 721–726.
- (28) Epping, J. D.; Chmelka, B. F. Nucleation and growth of zeolites and inorganic mesoporous solids: Molecular insights from magnetic resonance spectroscopy. *Curr. Opin. Colloid Interface Sci.* **2006**, *11*, 81–117.
- (29) Ciantar, M.; Mellot-Draznieks, C.; Nieto-Draghi, C. A Kinetic Monte Carlo Simulation Study of Synthesis Variables and Diffusion Coefficients in Early Stages of Silicate Oligomerization. *J. Phys. Chem. C* **2015**, *119*, 28871–28884.
- (30) Schmidt, J. E.; Fu, D. L.; Deem, M. W.; Weckhuysen, B. M. Template-Framework Interactions in Tetraethylammonium-Directed Zeolite Synthesis. *Angew. Chem., Int. Ed.* **2016**, *55*, 16044–16048.
- (31) Catlow, C. R. A.; Coombes, D. S.; Pereira, J. C. G. Computer modeling of nucleation, growth, and templating in hydrothermal synthesis. *Chem. Mater.* **1998**, *10*, 3249–3265.
- (32) Pereira, J. C. G.; Catlow, C. R. A.; Pereira, J. C. G.; Price, G. D. Silica condensation reaction: an *ab initio* study. *Chem. Commun.* **1998**, 1387–1388.
- (33) Pereira, J. C. G.; Catlow, C. R. A.; Price, G. D. *Ab initio* studies of silica-based clusters. Part I. Energies and conformations of simple clusters. *J. Phys. Chem. A* **1999**, *103*, 3252–3267.
- (34) Pereira, J. C. G.; Catlow, C. R. A.; Price, G. D. *Ab initio* studies of silica-based clusters. Part II. Structures and energies of complex clusters. *J. Phys. Chem. A* **1999**, *103*, 3268–3284.
- (35) Yang, C. S.; Mora-Fonz, J. M.; Catlow, C. R. A. Modeling the Polymerization of Aluminosilicate Clusters. *J. Phys. Chem. C* **2012**, *116*, 22121–22128.
- (36) Turrina, A.; Cox, P. A. Molecular Modelling of Structure Direction Phenomena. In *Insights into the Chemistry of Organic Structure-Directing Agents in the Synthesis of Zeolitic Materials*; Gómez-Hortigüela, L., Ed.; Springer International Publishing: Cham, 2018; pp. 75–102.
- (37) Ennaert, T.; Van Aelst, J.; Dijkmans, J.; De Clercq, R.; Schutyser, W.; Dusselier, M.; Verboekend, D.; Sels, B. F. Potential and challenges of zeolite chemistry in the catalytic conversion of biomass. *Chem. Soc. Rev.* **2016**, *45*, 584–611.
- (38) Dechnik, J.; Gascon, J.; Doonan, C. J.; Janiak, C.; Sumbly, C. J. Mixed-Matrix Membranes. *Angew. Chem., Int. Ed.* **2017**, *56*, 9292–9310.
- (39) Van Speybroeck, V.; Hemelsoet, K.; Joos, L.; Waroquier, M.; Bell, R. G.; Catlow, C. R. A. Advances in theory and their application within the field of zeolite chemistry. *Chem. Soc. Rev.* **2015**, *44*, 7044–7111.
- (40) Kirschhock, C. E. A.; Ravishankar, R.; Verspeurt, F.; Grobet, P. J.; Jacobs, P. A.; Martens, J. A. Identification of precursor species in the formation of MFI zeolite in the TPAOH-TEOS-H₂O system. *J. Phys. Chem. B* **1999**, *103*, 4965–4971.
- (41) Kirschhock, C. E. A.; Buschmann, V.; Kremer, S.; Ravishankar, R.; Houssin, C. J. Y.; Mojet, B. L.; van Santen, R. A.; Grobet, P. J.; Jacobs, P. A.; Martens, J. A. Zeosil nanoslabs: Building blocks in *n*Pr₄N⁺-mediated synthesis of MFI zeolite. *Angew. Chem., Int. Ed.* **2001**, *40*, 2637–2640.
- (42) Kirschhock, C. E. A.; Kremer, S. P. B.; Grobet, P. J.; Jacobs, P. A.; Martens, J. A. New evidence for precursor species in the formation of MFI zeolite in the tetrapropylammonium hydroxide-tetraethyl orthosilicate-water system. *J. Phys. Chem. B* **2002**, *106*, 4897–4900.
- (43) Kinrade, S. D.; Knight, C. T. G.; Pole, D. L.; Syvitski, R. T. Silicon-29 NMR studies of tetraalkylammonium silicate solutions. 1. Equilibria, Si-²⁹ chemical shifts, and Si-²⁹ relaxation. *Inorg. Chem.* **1998**, *37*, 4272–4277.
- (44) Kinrade, S. D.; Knight, C. T. G.; Pole, D. L.; Syvitski, R. T. Silicon-29 NMR studies of tetraalkylammonium silicate solutions. 2. Polymerization kinetics. *Inorg. Chem.* **1998**, *37*, 4278–4283.
- (45) Paris, C.; Moliner, M. Role of Supramolecular Chemistry During Templating Phenomenon in Zeolite Synthesis. In *Insights into the Chemistry of Organic Structure-Directing Agents in the Synthesis of Zeolitic Materials*; GomezHortigüela, L., Ed.; Springer: New York, 2018; pp. 139–177.
- (46) Rey, F.; Simancas, J. Beyond Nitrogen OSDAs. In *Insights into the Chemistry of Organic Structure-Directing Agents in the Synthesis of Zeolitic Materials*; GomezHortigüela, L., Ed.; Springer: New York, 2018; pp. 103–138.
- (47) Caratzoulas, S.; Vlachos, D. G.; Tsapatsis, M. On the role of tetramethylammonium cation and effects of solvent dynamics on the stability of the cage-like silicates Si₆O₁₅⁶⁻ and Si₈O₂₀⁸⁻ in aqueous solution. A molecular dynamics study. *J. Am. Chem. Soc.* **2006**, *128*, 596–606.
- (48) Mora-Fonz, M. J.; Catlow, C. R. A.; Lewis, D. W. H-Bond interactions between silicates and water during zeolite pre-nucleation. *Phys. Chem. Chem. Phys.* **2008**, *10*, 6571–6578.
- (49) Curtiss, L. A.; Frurip, D. J.; Blander, M. Studies of molecular association in H₂O and D₂O vapors by measurement of thermal-conductivity. *J. Chem. Phys.* **1979**, *71*, 2703–2711.
- (50) Xantheas, S. S.; Burnham, C. J.; Harrison, R. J. Development of transferable interaction models for water II. Accurate energetics of the first few water clusters from first principles. *J. Chem. Phys.* **2002**, *116*, 1493–1499.
- (51) Inada, Y.; Orita, H. Efficiency of numerical basis sets for predicting the binding energies of hydrogen bonded complexes: Evidence of small basis set superposition error compared to Gaussian basis sets. *J. Comput. Chem.* **2008**, *29*, 225–232.
- (52) Mora-Fonz, M. J.; Catlow, C. R. A.; Lewis, D. W. Oligomerization and cyclization processes in the nucleation of microporous silicas. *Angew. Chem., Int. Ed.* **2005**, *44*, 3082–3086.
- (53) Henschel, H.; Schneider, A. M.; Prosenic, M. H. Initial Steps of the Sol-Gel Process: Modeling Silicate Condensation in Basic Medium. *Chem. Mater.* **2010**, *22*, 5105–5111.
- (54) Becke, A. D. Density-functional thermochemistry III. The role of exact exchange. *J. Chem. Phys.* **1993**, *98*, 5648–5652.
- (55) Grimme, S. Semiempirical GGA-type density functional constructed with a long-range dispersion correction. *J. Comput. Chem.* **2006**, *27*, 1787–1799.
- (56) McNellis, E. R.; Meyer, J.; Reuter, K. Azobenzene at coinage metal surfaces: Role of dispersive van der Waals interactions. *Phys. Rev. B* **2009**, *80*, 205414.
- (57) Becke, A. D. A multicenter numerical-integration scheme for polyatomic-molecules. *J. Chem. Phys.* **1988**, *88*, 2547–2553.
- (58) Lee, C.; Yang, W.; Parr, R. G. Development of the colle-savetti correlation-energy formula into a functional of the electron-density. *Phys. Rev. B* **1988**, *37*, 785–789.
- (59) Mehandzhyski, A. Y.; Riccardi, E.; van Erp, T. S.; Trinh, T. T.; Grimes, B. A. *Ab Initio* Molecular Dynamics Study on the Interactions between Carboxylate Ions and Metal Ions in Water. *J. Phys. Chem. B* **2015**, *119*, 10710–10719.
- (60) Szyja, B. M.; Vassilev, P.; Trinh, T. T.; van Santen, R. A.; Hensen, E. J. M. The relative stability of zeolite precursor tetraalkylammonium-silicate oligomer complexes. *Microporous Mesoporous Mater.* **2011**, *146*, 82–87.
- (61) Trinh, T. T.; Jansen, A. P. J.; van Santen, R. A.; Meijer, E. J. Role of Water in Silica Oligomerization. *J. Phys. Chem. C* **2009**, *113*, 2647–2652.

- (62) Trinh, T. T.; Jansen, A. P. J.; van Santen, R. A.; Meijer, E. J. The role of water in silicate oligomerization reaction. *Phys.Chem.-Chem.Phys.* **2009**, *11*, 5092–5099.
- (63) Zhang, X.-Q.; Trinh, T. T.; van Santen, R. A.; Jansen, A. P. J. Mechanism of the Initial Stage of Silicate Oligomerization. *J. Am. Chem. Soc.* **2011**, *133*, 6613–6625.
- (64) Klamt, A.; Schuurmann, G. COSMO: A new approach to dielectric screening in solvents with explicit expressions for the screening energy and its gradient. *J. Chem. Soc., Perkin Trans. 2* **1993**, 799–805.
- (65) Baldrige, K.; Klamt, A. First principles implementation of solvent effects without outlying charge error. *J. Chem. Phys.* **1997**, *106*, 6622–6633.
- (66) Andzelm, J.; Kölmel, C.; Klamt, A. Incorporation of solvent effects into density-functional calculations of molecular-energies and geometries. *J. Chem. Phys.* **1995**, *103*, 9312–9320.
- (67) Govind, N.; Petersen, M.; Fitzgerald, G.; King-Smith, D.; Andzelm, J. A generalized synchronous transit method for transition state location. *Comput. Mater. Sci.* **2003**, *28*, 250–258.
- (68) Kelly, C. P.; Cramer, C. J.; Truhlar, D. G. SM6: A density functional theory continuum solvation model for calculating aqueous solvation free energies of neutrals, ions, and solute-water clusters. *J. Chem. Theory Comput.* **2005**, *1*, 1133–1152.
- (69) Hirano, T. A note on thermochemistry. In *MOPAC Manual*; MOPAC: Stewart, J. J. P., Ed.; 1993; pp. 71–77.
- (70) Delley, B. An all-electron numerical-method for solving the local density functional for polyatomic-molecules. *J. Chem. Phys.* **1990**, *92*, 508–517.
- (71) Delley, B. From molecules to solids with the DMol³ approach. *J. Chem. Phys.* **2000**, *113*, 7756–7764.